Reactivity of Ester Linkages and Pentaammineruthenium(III) at the Monolayer Assembly/Solution Interface

ARTICLE *in* LANGMUIR · DECEMBER 1996

Impact Factor: 4.46 · DOI: 10.1021/la960027p

9 AUTHORS, INCLUDING:

Hal Van Ryswyk
Harvey Mudd College
24 PUBLICATIONS **576** CITATIONS
SEE PROFILE

Tobias Herman
Montgomery College
23 PUBLICATIONS **260** CITATIONS
SEE PROFILE

Reactivity of Ester Linkages and Pentaammineruthenium(III) at the Monolayer Assembly/ Solution Interface

Hal Van Ryswyk,* Eric D. Turtle, Rachel Watson-Clark, Troy A. Tanzer, Tobias K. Herman, Pek Yoke Chong, Petra J. Waller, Aaron L. Taurog, and Carl E. Wagner

Department of Chemistry, Harvey Mudd College, Claremont, California 91711-5990

Received January 9, 1996[⊗]

The rate of base-mediated ester hydrolysis in monolayers of 11-mercaptoundecyl isonicotinate on gold is monitored by infrared spectroscopy and cyclic voltammetry. The hydrolysis product, a surface-confined alcohol, can be converted to a trifluoroacetate, increasing the sensitivity of infrared monitoring. Pentaammineruthenium(II) can be attached to the pendant isonicotinate either prior to or after monolayer assembly, leading to monolayers with a highly-charged monolayer/solution interface and a built-in electrochemical probe. The rate of ester hydrolysis within the monolayer is controlled by steric factors associated with monolayer packing and by the amount of charge at the monolayer/solution interface. The stability of the pendant Ru(III) complex is very sensitive to pH and interfacial charge. These results are correlated with Gouy−Chapman double-layer theory.

Introduction

Monolayer assemblies provide excellent model systems for the study of interfacial processes. Proton, electron, and energy transfer and wetting, friction, and chemical sensing studies all benefit from the extreme orderliness provided by self-assembling monolayers. *In-situ* chemical transformation of the monolayer surface group can provide more varied model systems via the introduction of new chemical functionality into monolayer assemblies, lend lateral control to surface group functionality, or serve as an anchor for the formation of multilayer structures. Sulfate and phosphate surface groups have been introduced into monolayers of 11-mercaptoundecanol as a prelude to biological complexation.[1] Monolayers of carboxylic acids have been converted to acid halides and then to various amides and esters.[2] Esterification based on carbodiimide reagents provides a convenient way to functionalize monolayers;[3] transesterification is another attractive strategy to alter interfacial chemical properties.[4] Monolayers of aryl azides can be modified photochemically through masks to form two-dimensional patterns of various azepine derivatives,[5] and ligands can be inserted into the coordination sphere of pendant manganese carbonyls.[6] Scanning electron microscopy can be used to selectively modify monolayers.[7] Multilayer structures can be built upon alkanethiol monolayers by reacting derivatized silanes with hydroxide surface groups[8] and via ionic bonding of phosphate surface groups with metal ions.[9]

The majority of these studies use monolayer derivatization as a means to some end. Only a handful of studies address the changes in functional group reactivity upon incorporation within the monolayer/solution interface. In many cases, the reactivity of functional groups may change substantially upon monolayer incorporation. In an elegant series of papers, Maoz and Sagiv[10] used attenuated-total-reflectance infrared spectroscopy to monitor the rate of permanganate-based oxidation of unsaturated alkylsilane monolayers. They showed the rate of these reactions to be ion penetration-controlled, influenced largely by the overall structure, packing, and orderliness of the underlying monolayer assembly.

In addition to packing considerations, reactivity at the monolayer/solution interface can be influenced by charge. Recent studies address the influence of charge at the monolayer/solution interface on the thermodynamics[11] and kinetics[12] of electron transfer to pendant electroactive groups, but no studies to date address the effects of charge residing at the interface upon the reactivity of surface-confined functional groups.

Our goal in the present study is to further investigate factors influencing the reactivity of functional groups at the monolayer/solution interface. A better understanding of the factors influencing interfacial reactivity not only would better inform the design of future model systems but also would underpin the rational design of multilayer systems and chemical sensors. Specifically, we seek to understand the influence of monolayer structure and charge localized at the monolayer/solution interface on a simple reaction, the base-mediated hydrolysis of esters. In these studies monolayers of 11-mercaptoundecyl isonicotinate (MUIN) provide a self-assembling alkanethiol

* To whom correspondence should be addressed. Telephone: (909) 607-3908. Fax: (909) 607-7577. E-mail:Hal_VanRyswyk@hmc.edu.

[⊗] Abstract published in *Advance ACS Abstracts,* November 15, 1996.

(1) Bertilsson, L.; Liedberg, B. *Langmuir* **1993**, *9*, 141.

(2) (a) Duevel, R. V.; Corn, R. M. *Anal. Chem.* **1992**, *64*, 337. (b) Keller, H.; Schrepp, W.; Fuchs, H. *Thin Solid Films* **1992**, *210*, 799.

(3) Katz, E.; Itzhak, N.; Willner, I. *Langmuir* **1993**, *9*, 1392.

(4) Neogi, P.; Neogi, S.; Stirling, C. J. M. *J. Chem. Soc., Chem. Commun.* **1993**, 1134.

(5) (a) Wollman, E. W.; Kang, D.; Frisbie, C. D.; Lorkovic, I. M.; Wrighton, M. S. *J. Am. Chem. Soc.* **1994**, *116*, 4395. (b) Frisbie, C. D.; Wollman, E. W.; Wrighton, M. S. *Langmuir* **1995**, *11*, 2563. (c) Frisbie, C. D.; Wollman, E. W.; Martin, J. R.; Wrighton, M. S. *J. Vac. Sci. Technol., A* **1993**, *11*, 2368. (d) Frisbie, C. D.; Wollman, E. W.; Wrighton, M. S. *Langmuir* **1993**, *9*, 1517. (e) Rozsnyai, L. F.; Wrighton, M. S. *Langmuir* **1995**, *11*, 3913.

(6) Kang, D.; Wrighton, M. S. *Langmuir* **1991**, *7*, 2169.

(7) Lopez, G. P.; Biebuyck, H. A.; Whitesides, G. M. *Langmuir* **1993**, *9*, 1513.

(8) Ulman, A.; Tillman, N. *Langmuir* **1989**, *5*, 1418.

(9) (a) Keller, S. W.; Kim, H.-N.; Mallouk, T. E. *J. Am. Chem. Soc.* **1994**, *116*, 8817. (b) Cao, G.; Hong, H. G.; Mallouk, T. E. *Acc. Chem. Res.* **1992**, *25*, 420. (c) Hong, H. G.; Mallouk, T. E. *Langmuir* **1991**, *7*, 2362.

(10) (a) Maoz, R.; Sagiv, J. *Langmuir* **1987**, *3*, 1034. (b) Maoz, R.; Sagiv, J. *Langmuir* **1987**, *3*, 1045. (c) Maoz, R.; Sagiv, J. *Thin Solid Films* **1985**, *132*, 135.

(11) Redepenning, J.; Tunison, H. M.; Finklea, H. O. *Langmuir* **1993**, *9*, 1404.

(12) Creager, S. E.; Weber, K. *Langmuir* **1993**, *9*, 844.

S0743-7463(96)00027-3 CCC: $12.00

Scheme 1. Surface-Confined MUIN Diluted in Decanethiol Undergoing Base-Mediated Hydrolysis

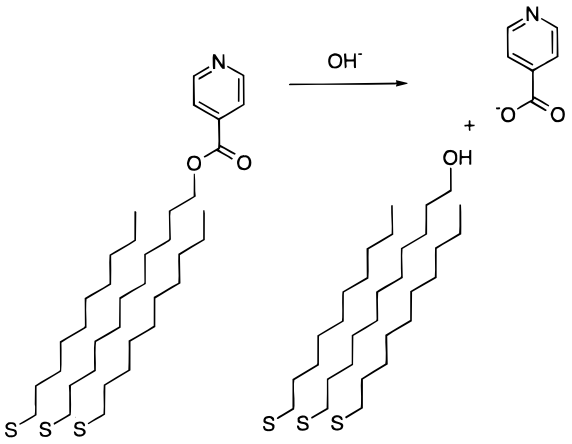

system with a labile ester functionality and the potential for coordination with hydrophilic redox centers. Scheme 1 shows MUIN diluted in decanethiol undergoing base-mediated hydrolysis. As shown below, the rate of ester hydrolysis can be studied as a function of monolayer packing; the effect of interfacial charge on the hydrolysis rate can be studied by attaching pentaammineruthenium-(II) to the pendant isonicotinate to form a charged monolayer while simultaneously affording an *in-situ* electrochemical tag for monitoring hydrolysis.

Experimental Section

Materials. Absolute ethanol was used as received from USI Chemicals. Unless otherwise noted, all other chemicals were obtained from Aldrich Chemical and used as received.

11-Thioacetylundecanol. 11-Bromoundecanol (10 g, 40 mmol) was stirred with potassium thioacetate (9.1 g, 80 mmol) in methanol at reflux for 10 h under nitrogen. After the reaction mixture was cooled to room temperature, it was poured into aqueous ammonium chloride and extracted three times with diethyl ether. Solvent was removed *in vacuo* and the residue dissolved in hexane and precipitated by addition of diethyl ether to obtain 7 g (85%) of product. IR (THF, cm^{-1}): (C═O) 1690. ^1H NMR ($CDCl_3$, δ): 3.64 (t, 2H, $J = 6.3$ Hz), 2.85 (t, 2H, $J = 6.3$ Hz), 2.3 (s, 3H), 1.5−1.0 (m, 18H).

11-Mercaptoundecanol. 11-Thioacetylundecanol (2.46 g, 10 mmol) was added to a slurry of sodium bicarbonate (2.52 g, 30 mmol) in 75 mL of dry, degassed methanol and allowed to stir at room temperature for 3 h. The reaction was quenched with 50 mL of saturated aqueous ammonium chloride, and extracted three times with 30 mL of diethyl ether. The extract was dried over magnesium sulfate and the solvent removed *in vacuo*. ^1H NMR ($CDCl_3$, δ): 3.64 (t, 2H, $J = 6.3$ Hz), 2.5 (q, 2H, $J = 6$ Hz), 1.5−1.0 (m, 18H).

4-Pyridinecarbonyl Chloride. Isonicotinic acid (Eastman Kodak) (5 g, 40 mmol) was dissolved in 25 mL of thionyl chloride and refluxed for 3 h. Thionyl chloride was removed *in vacuo*, leaving a lime-green solid.

11-Bromoundecyl Isonicotinate. 4-Pyridinecarbonyl chloride (4 g, 28 mmol) and 11-bromoundecanol (7 g, 28 mmol) were refluxed in 85 mL of benzene for 3 h. After the reaction mixture was cooled to room temperature, 160 mL of chloroform was added. The mixture was washed three times with 30 mL of saturated aqueous sodium bicarbonate and once with water and then dried over sodium sulfate. The solvent was removed and the residue recrystallized from benzene. ^1H NMR ($CDCl_3$, δ): 8.8 (d, 2H, $J = 6.1$ Hz), 7.8 (d, 2H, $J = 6.1$ Hz), 4.37 (t, 2H, $J = 6.7$ Hz), 3.36 (t, 2H, $J = 6.3$ Hz), 1.9−1.1 (m, 18H).

11-Mercaptoundecyl Isonicotinate. Sodium (0.5 g, 21 mmol) was added to 25 mL of absolute ethanol and the solution cooled to room temperature. The solution was saturated with hydrogen sulfide gas for 10 min (excess hydrogen sulfide was trapped in a 5 M KOH solution). 11-Bromoundecyl isonicotinate (3.36 g, 9.76 mmol) in 25 mL of ethanol was added dropwise over 5 min, and the mixture was refluxed for 10 min while maintaining hydrogen sulfide saturation. The mixture was allowed to cool for 5 min prior to addition of ammonium chloride (3 g, 56 mmol) in 60 mL of water. The mixture was extracted three times with 20 mL of dichloromethane and the organic layer dried over sodium sulfate. Recrystallization from toluene and methanol yielded a white solid. IR (CCl_4, cm^{-1}): (C═O) 1732, (C−O) 1279. ^1H NMR ($CDCl_3$, δ): 8.8 (d, 2H, $J = 6.1$ Hz), 7.8 (d, 2H, $J = 6.1$ Hz), 4.37 (t, 2H, $J = 6.7$ Hz), 2.5 (q, 2H, $J = 6$ Hz), 1.75 (m, 2H), 1.63 (m, 2H), 1.34 (m, 14H).

Bis(11-hydroxyundecyl) Disulfide. 11-Thioacetylundecanol (2 g, 8.1 mmol) was stirred in 25 mL of ethanolic KOH (0.91 g, 16.2 mmol) until a cloudy precipitate formed; 2.0 mL of 30% H_2O_2 (18.0 mmol) was added and the cloudy solution heated to 80 °C for 3 h. The cooled mixture was poured into water, extracted with diethyl ether, and dried over sodium sulfate. Evaporation of the solvent and recrystallization from benzene yielded a white solid. Mp: 78−80 °C. ^1H NMR ($CDCl_3$, δ): 3.64 (t, 4H, $J = 6.3$ Hz), 2.68 (t, 4H, $J = 6.3$ Hz), 1.65 (m, 4H, $J = 6.3$ Hz), 1.4−1.1 (m, 32H).

Bis[11-((pyridinylcarbonyl)oxy)undecyl] Disulfide. Bis-(11-hydroxyundecyl) disulfide (1 g, 4.2 mmol) was added to 4-pyridinecarbonyl chloride (1.1 g, 8.4 mmol) and 1 equiv of triethylamine in toluene and refluxed for 3 h. The solvent was removed *in vacuo*, and the residue recrystallization from toluene and methanol yielded a white solid. IR (CCl_4, cm^{-1}): (C═O) 1732, (C−O) 1279. ^1H NMR ($CDCl_3$, δ): 8.8 (d, 4H, $J = 11$ Hz), 6.64 (d, 4H, $J = 11$ Hz), 4.28 (t, 4H, $J = 6$ Hz), 2.68 (t, 4H, $J = 6$ Hz), 1.75 (m, 4H), 1.63 (m, 4H), 1.34 (m, 28H).

4-(12-Bromododecyl)pyridine. Diisopropylamine (0.64 g, 6.4 mmol) and *n*-butyllithium in hexane (6.4 mmol) were added to 3 mL of THF in a nitrogen-purged Schlenk flask and allowed to react for 15 min. The mixture was transferred dropwise over 30 min via canula to a second Schlenk flask containing 4-methylpyridine (596 mg, 6.4 mmol). The contents were allowed to stir for 30 min. This mixture was transferred dropwise over 15 min via cannula to a stirred solution of 1,11-dibromoundecane (2.01 g, 6.4 mmol) in THF at 0 °C. The reaction was allowed to warm to room temperature. After 90 min, 25 mL of ice water was added, producing a two-phase system. The THF layer was retained, and the aqueous layer was extracted three times with 30 mL of diethyl ether. The organic layers were combined and dried over sodium sulfate. Solvent was removed *in vacuo* and the crude product purified by Kugelrohr distillation and recrystallization from ethyl acetate. ^1H NMR ($CDCl_3$, δ): 8.47 (d, 2H, $J = 6$ Hz), 7.10 (d, 2H, $J = 6$ Hz), 3.36 (t, 2H, $J = 6.8$ Hz), 2.60 (t, 2H, $J = 7.3$ Hz), 2.0−1.2 (m, 20H).

4-(12-Thioacetyldodecyl)pyridine was produced in a fashion analogous to that for 11-thioacetylundecanol. ^1H NMR ($CDCl_3$, δ): 8.47 (d, 2H, $J = 6$ Hz), 7.10 (d, 2H, $J = 6$ Hz), 2.85 (t, 2H, $J = 6.3$ Hz), 2.60 (t, 2H, $J = 7.3$ Hz), 2.3 (s, 3H), 2.0−1.2 (m, 20H).

4-(12-Mercaptododecyl)pyridine was produced in a fashion analogous to that for 11-mercaptoundecanol. ^1H NMR ($CDCl_3$, δ): 8.47 (d, 2H, $J = 6$ Hz), 7.10 (d, 2H, $J = 6$ Hz), 2.60 (t, 2H, 7.3 Hz), 2.5 (q, 2H, $J = 6$ Hz), 2.0−1.2 (m, 20H).

Hexaammineruthenium(III) chloride was obtained from Strem Chemicals. Chloropentaammineruthenium(III) chloride[13] and pentaammineaquoruthenium(II) hexafluorophosphate[14] were prepared via literature methods; the later product was stored in an argon-filled drybox equipped with a Vacuum Atmospheres HE-493 dri-train.

Electrodes were either polycrystalline 0.5 mm diameter gold wire (Aldrich, 99.99%) or gold mirrors. Gold mirrors were fabricated via thermal evaporation of 50 Å of titanium, followed by 2000 Å of gold (Johnson Matthey, 99.99%), onto a silicon ⟨100⟩ wafer (Silicon Quest International) which had first been cleaned via the RCA etch (10 min at 100 °C in 5:1:1 water/concentrated ammonium hydroxide/30% hydrogen peroxide). Gold wires were either flame annealed[11] or etched for 10 s in hot "piranha" solution (1:4 30% hydrogen peroxide/concentrated sulfuric acid. **CAUTION**: *piranha solution reacts violently with most organic materials and should be handled with extreme care*); gold mirrors were either etched in piranha solution or plasma etched (200

(13) Vogt, L. H.; Katz, J. L.; Wiberley, S. B. *Inorg. Chem.* **1965**, *4*, 1157.

(14) Kuehn, C. G.; Taube, H. *J. Am. Chem. Soc.* **1976**, *98*, 689.

mTorr of O_2 for 2 min, then 400 mTorr of H_2 for 4 min, at 100 W total radio frequency power in a Harrick PDC-32G plasma cleaner). Electrodes were immersed immediately in deposition solutions after cleaning. All deposition solutions were 0.1 mM total thiol or disulfide, unless otherwise noted. Deposition times were typically 16 h.

Monolayers of ruthenium-terminated MUIN were formed in two ways. Ruthenium could be attached to monolayers of MUIN by placing monolayers in 2 mL of THF containing $[Ru(NH_3)_5(OH_2)](PF_6)_2$ (5 mg, 0.014 mmol) for 3 h in an argon-purged glovebox. The monolayers were removed from the glovebox and deposition solution, rinsed with THF and then water, and used immediately. Alternatively, $[Ru(NH_3)_5(OH_2)](PF_6)_2$ (2.5 mg, 0.007 mmol) could be dissolved in a 1mM solution of MUIN in THF (5 mL, 0.005 mmol) and left to stand for 3 min prior to introduction of freshly-etched gold substrates. Deposition times were typically 3 h, followed by sequential rinsing in THF and water, and immediate use.

Buffer solutions were 0.01 M in buffer capacity and were prepared as follows: pH 2−3 phosphoric acid/sodium dihydrogen phosphate; pH 4−5 acetic acid/sodium acetate; pH 6−8 sodium dihydrogen phosphate/sodium hydrogen phosphate; pH 9−11 sodium hydrogen carbonate/sodium carbonate. Exact pH values were determined with a Cole-Parmer 5996−50 pH meter and a VWR Scientific 34100 pH electrode, using calibration buffers from EM Science traceable to SRM 186 I and II.

Infrared Reflection−Absorption Spectroscopy. Grazing angle reflection−absorption infrared spectroscopy was performed with a Mattson Galaxy 5020 spectrometer equipped with a Specac "seagull" specular reflectance accessory and a liquid-nitrogen-cooled mercury-cadmium-telluride detector. The angle of incidence for the p-polarized light was 80° from the surface normal. Spectra were typically recorded using 2000 scans at 4 cm^{-1} resolution. The detector, optics, and custom-built glovebag about the sample chamber of the spectrometer were purged with air from a Balston 75-52 FTIR purge gas generator (dew point −73 °C).

Trifluoroacetic Anhydride Tagging. Monolayer-coated samples were placed in 10 mL of freshly-distilled THF (from sodium/benzophenone under argon) and sealed in a Schlenk tube under argon. Trifluoroacetic anhydride (PCR Research Chemicals) (0.3 mL, 2.1 mmol) and triethylamine (Sigma) (0.3 mL, 2.1 mmol) were injected via syringe, and the tube was allowed to stand for 1 h.[1] After reaction was complete, the samples were rinsed with THF and then ethanol, dried under a stream of argon, and then evacuated to 0.1 Torr for 1 h. The samples were transferred to the sample compartment of the FTIR *in vacuo*, where they were placed on the sampling stage without coming into contact with ambient air.

Contact Angle Titrations. Contact angle titrations were performed in the "nonreactive spreading" mode[15] with an apparatus assembled in our laboratory. Under this protocol, samples were removed from the deposition solution, rinsed with ethanol and deionized water, dried under an argon stream, and then immersed in the buffer solution to be used to measure the contact angle. After removal from the buffer solution, any adhering water droplets were blown off the surface with an argon stream, and the sample was mounted in the goniometer. Measurements were made under ambient conditions, using green light to illuminate the water droplet. All values reported are advancing contact angles, obtained by expanding a droplet from a microliter syringe until it advances smoothly across the surface and then measuring the contact angle 10−30 s after expansion. Contact angles measured in this fashion were invariant (±1°) on a time scale of several minutes. Each value reported is the average of the values for three samples.

Ellipsometry. Ellipsometry was performed with a Gaertner ellipsometer employing a 632.8 nm light source at 70° incidence. Clean gold mirrors were soaked in 10 mM solutions of ethanethiol in ethanol for 30 min, rinsed in ethanol, blown dry with Ar, and then measured for optical null. Monolayers of MUIN were assembled on these mirrors over 17 h, rinsed, and dried, and the optical null was measured again. Thickness calculations used a monolayer refractive index of 1.45.

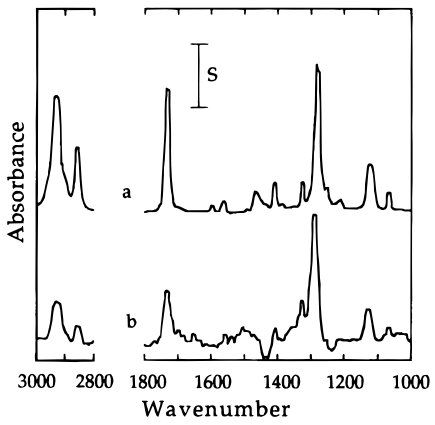

Figure 1. (a) Infrared absorption spectrum of 17.7 mM MUIN in carbon tetrachloride solution: cell path length, 0.2 mm; $S = 0.1$ A. (b) Infrared reflection−absorption spectrum of MUIN on gold: $S = 1.6 \times 10^{-3}$ A.

Cyclic Voltammetry. Reductive stripping of monolayer-coated samples was performed in argon-purged 1 M KOH, in a sealed cell. Surface coverages were determined either by cut-and-weigh techniques or via EG&G 270 electrochemical software-based integration. Fractional surface coverage measurements were done in a 5 mM solution of either $K_3Fe(CN)_6$ or $K_4Fe(CN)_6$ in 1.0 M KCl at pH ranging from 3 to 8. Cyclic voltammetry of ruthenium-tagged monolayers was performed in 0.1 M Na_2SO_4 adjusted to pH 4.

AC Impedance Spectroscopy. AC impedance spectroscopy was performed with an EG&G 263 potentiostat, a 5210 lock-in amplifier, and 398 software. The electrolyte was equimolar $K_3Fe(CN)_6$ and $K_4Fe(CN)_6$ (5 mM) in 1.0 M KCl, with the dc potential set to the formal potential of the redox couple and an ac potential of 5 mV root mean square.

Hydrolysis Monitoring. Hydrolysis rate constants were determined via cyclic voltammetry in a sealed, argon-purged cell, containing the fixed, monolayer-covered working electrode, a platinum counter electrode, and a silver quasi-reference electrode. The cell was constructed so that electrolyte could be drained from the bottom and precisely 2.0 mL of either 0.1 M Na_2SO_4 adjusted to pH 4 or pH 10 buffer solution could be added while keeping the cell under argon purge. The immersed electrode area was constant within 2%, as determined by measurement of electroactive ruthenium in successive runs interspersed by draining, rinsing, and refilling the cell.

Results and Discussion

Characterization of MUIN Monolayers. Monolayers of 11-mercaptoundecyl isonicotinate (MUIN) can be formed by overnight deposition from 0.1 mM solutions of either the thiol or disulfide in ethanol. Grazing angle reflection−absorption infrared spectroscopy provides information regarding the orientation of the monolayer. General inferences regarding monolayer orientation can be made with reference to the IR surface selection rule: the specular reflectance experiment is sensitive only to those bands with components of the transition dipole which project onto the surface normal.[16] Figure 1 shows the methylene-stretching region of the MUIN monolayer spectrum. The broad, antisymmetric methylene-stretching band located at 2928 cm^{-1} indicates a disordered, liquid-like structure for the alkane chains. In monolayers with crystal-like order, such as longer-chain alkanethiols without bulky surface groups, this band moves toward 2918 cm^{-1}. The 35 cm^{-1} fwhm of the methylene antisymmetric stretching peak is significantly larger than that of undecanethiol (19 cm^{-1}), indicating an ensemble of

(15) Creager, S. E.; Clarke, J. *Langmuir* **1994**, *10*, 3675.

(16) Greenler, R. G. *J. Phys. Chem.* **1966**, *44*, 310.

MUIN chain alignments.[17] The degree of disorder indicated by the position of the antisymmetric band and its breadth is similar to that of other C_{11} alkanethiol monolayers with large surface groups. For example, monolayers of 11-mercaptoundecanoic acid[2a] show a peak maxima at 2924 cm^{-1} with a fwhm of 33 cm^{-1}. Taking account for the variation in the angle of incidence between experiments,[18] the area under the MUIN methylene bands is similar to that observed for $R(CH_2)_{11}SH$, where R = (η^5-C_5H_5)Fe(η^5-C_5H_4)CO_2,[19] NC, HOOC, and HO, but considerably more than that observed in unsubstituted undecanethiol monolayers. The alkane chain tilt angle in unsubstituted alkanethiols has been calculated at 27°. The introduction of a small amount of chain disorder into such highly-ordered systems leads to larger methylene mode intensities; for totally disordered chains a limiting tilt angle of 35.3° is calculated.[17] Alternatively, a well-ordered system with a larger tilt angle would also produce larger methylene mode intensities. Given the indications of alkane chain disorder in the MUIN system, our calculated chain tilt angle of 33° is heavily influenced by this disorder and should be regarded as an upper bound.

Notwithstanding the disorder in the alkane chain, comparisons of molecular orientation are still possible. The solution-phase infrared spectrum of MUIN is contrasted with that of the monolayer in Figure 1. The methylene stretches and the carbonyl stretching band at 1734 cm^{-1} in the monolayer are foreshortened relative to the ester C−O stretch at 1288 cm^{-1}. This is consistent with the axes of the alkane chains and the carbonyl tilting off normal, while the longitudinal ester stretch is aligned normal to the surface. Further support of this orientation is provided by an examination of the isonicotinate ring modes. The major ring modes present in the monolayer spectrum (18a, 19a, 19b)[20] are those with a transition dipole along the major axis of the molecule. These bands would be observed in orientations where the long axis of the isonicotinate ring projects onto the surface normal.

Ellipsometric measurements of four samples show a monolayer thickness of 21.4 ± 1.8 Å, which compares with a maximum thickness of 23 Å for MUIN with a fully-extended alkane chain oriented perpendicular to the surface. This thickness is consistent with those found for other monolayers with 11−16 carbon alkane chains.[17,18] In general, ellipsometric measurements of monolayer thickness provide values which are somewhat larger than those based on infrared-based molecular orientation calculations.[17]

An estimate of surface coverage, based upon the cross-sectional area of the isonicotinate surface group and informed by accepted surface coverages of 8×10^{-10} mol cm^{-2} for octadecanethiol and 4×10^{-10} mol cm^{-2} for monolayers with ferrocenyl surface groups, would place Γ_{MUIN} around 6×10^{-10} mol cm^{-2}. Monolayers composed of MUIN in small mole fraction with decanethiol would most likely form mixed monolayers such as the one illustrated in Scheme 1, wherein the overall packing and geometry of the monolayer are determined by the decanethiol diluent.[21]

The open fraction of the surface area, $1 - \theta$, as determined by ac impedance[22] for a freshly-assembled monolayer of MUIN, is $(1.5 \pm 0.6) \times 10^{-3}$. Cyclic voltammograms of $Fe(CN)_6^{3-}$ using a MUIN-coated electrode show no identifiable peak or plateau. The value of $1 - \theta$ calculated for this system is quite similar to that of a freshly-assembled octadecanethiol monolayer. While the C_{11} chain is disordered, as shown by IR spectroscopy, the isonicotinate overlayer is quite effective in blocking ion penetration. Put differently, the C_{11} MUIN monolayer is as effective in blocking charge penetration as a more highly ordered, thicker C_{18} system.[22]

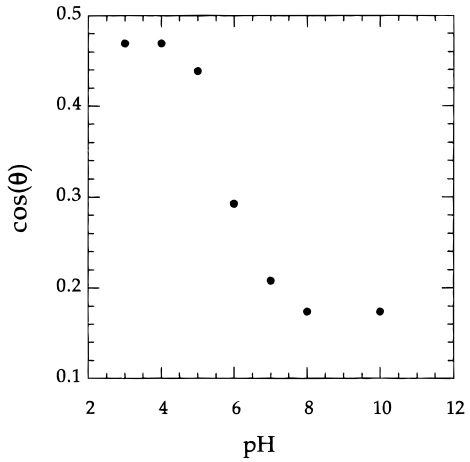

Figure 2. Contact angle titration curve for a MUIN monolayer using the nonreactive spreading protocol. Experimental details are in the text.

Recent advances in contact angle titrations,[23] using a nonreactive spreading technique, allow direct observation of pK_a values for surface-confined species.[15] The results of such an experiment on a monolayer of MUIN are shown in Figure 2. At low pH values, the protonation of the exposed pyridine residue yields a surface which is more easily wetted, whereas, at higher pH values, the exposed, deprotonated pyridine residue is not wetted as well. The pK_a for the surface-confined pyridine residue is approximately 5.5, which compares to a pK_a of 3.26 for methyl isonicotinate in aqueous solution.[24] A positive two-unit shift in pK_a is consistent with other examples of monolayer-confined acids. Monolayers of 4-mercaptopyridine show a pK_a of 4.6 at the point of zero charge (pzc) on gold,[25] versus 1.4 in bulk.[26] Monolayers of 4-aminothiophenol show a pK_a of 6.9 at the pzc on gold, versus 4.3 in the bulk phase.[25] Monolayers of 11-mercaptoundecanoic acid diluted 1:1 in nonanethiol show a pK_a of 6.5, versus 4.8 in the bulk phase.[15] In each of these cases, the magnitude and direction of the shift in pK_a are the same, regardless of whether the surface is becoming charged or uncharged with increasing pH. Similar effects are observed in micelles and lipid bilayers.[27]

The state of monolayer protonation has little effect on the electrochemical blocking properties of MUIN monolayers; values of $1 - \theta$, as measured by ac impedance spectroscopy, were constant over the range of pH 3−8.

There is evidence of multilayer formation at deposition concentrations greater than 10 mM in ethanol. In such cases, the intensity of the methylene stretching bands increases as much as 20-fold, while the lower frequency peaks increase only 5-fold. The only prominent isonico-

(17) Porter, M. D.; Bright, T. B.; Allara, D. L.; Chidsey, C. E. D. *J. Am. Chem. Soc.* **1987**, *109*, 3559.
(18) Chidsey, C. E. D.; Loiacono, D. N. *Langmuir* **1990**, *6*, 682.
(19) Sato, Y.; Frey, B. L.; Corn, R. M.; Uosaki, K. *Bull. Chem. Soc. Jpn.* **1994**, *25*, 21.
(20) (a) Lord, R. C.; Marston, A. L.; Miller, F. A. *Spectrochim. Acta* **1957**, *79*, 113. (b) Spinner, E. *J. Phys. Chem.* **1988**, *92*, 3379.
(21) Chidsey, C. E. D. *Science* **1991**, *251*, 919.
(22) Finklea, H. O.; Snider, D. A.; Fedyk, J.; Sabatani, E.; Gafni, Y.; Rubinstein, I. *Langmuir* **1993**, *9*, 3660.
(23) Whitesides, G. M.; Paibinis, P. E. *Langmuir* **1990**, *6*, 87 and references therein.
(24) Green, R. W.; Tong, H. K. *J. Am. Chem. Soc.* **1956**, *78*, 4896.
(25) Bryant, M. A.; Crooks, R. M. *Langmuir* **1993**, *9*, 385.
(26) Albert, A.; Barlin, G. B. *J. Chem. Soc.* **1959**, *56*, 2384.
(27) (a) Goddard, E. D. *Adv. Colloid Interface Sci.* **1974**, *4*, 45. (b) Fernandez, M. S.; Fromherz, P. *J. Chem. Phys.* **1977**, *81*, 1755.

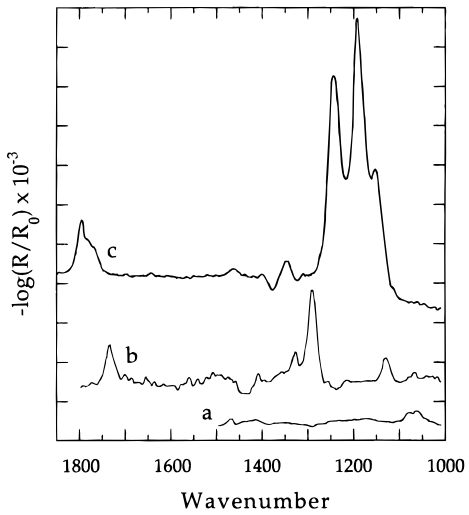

Figure 3. Mid-infrared region reflection−absorption spectra of (a) 11-mercaptoundecanol, (b) MUIN, and (c) 11-mercaptoundecyl trifluoroacetate.

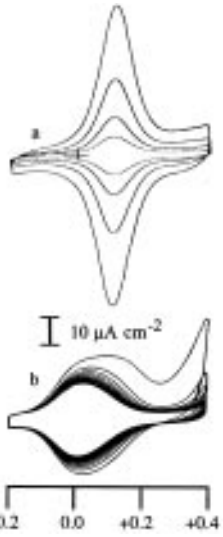

Figure 4. Cyclic voltammograms of a MUIN monolayer tagged with pentaammineruthenium(II) prior to self-assembly, $\Gamma_{Ru} = 2.0 \times 10^{-10}$ mol cm^{-2}: (a) scan rates of 50, 100, 200, and 400 mV s^{-1} at pH 4.0 versus SCE; (b) sequential scans at 400 mV s^{-1} in pH 10.0 buffer versus silver quasi-reference electrode.

tinate ring mode is that at 1456 cm^{-1}. In multilayer adsorption, it appears that the isonicotinate rings and ester moieties in subsequent monolayers are oriented largely parallel to the surface, whereas the alkane chain tends toward a perpendicular alignment. Electrochemical evidence for multilayer adsorption at high deposition solution concentrations is discussed below.

From the evidence presented, the following picture of the MUIN monolayer emerges: the monolayer is compact and efficient at blocking ion access to the underlying gold. Overall surface coverage is on the order of 6×10^{-10} mol cm^{-2}. The alkane chains are extended and tilted, but there is considerable disorder, most likely due to steric interactions of the isonicotinate surface groups. The isonicotinates stand erect, with at least some of the pyridine residues accessible to the supernatant solution. The interaction of the pyridine residues with their neighbors has increased the pK_a to 5.5.

Monolayer Tagging. Grazing angle reflection−absorption infrared spectroscopy is an attractive method for following reactions at the monolayer/solution interface. Unfortunately, as illustrated in Figure 3, the surface-confined alcohol resulting from the base-mediated hydrolysis of MUIN has a very weak spectral signature. The sensitivity to hydrolysis products can be enhanced if the surface-confined alcohol is reacted with trifluoroacetic anhydride (TFAA), producing a surface-confined trifluoroacetate.[1] The strength of the resulting $\nu(CF_2)(a')$, $\nu(CF_3)(a')$, and $\nu(CF_2)(a'')$ stretching modes, at 1250, 1197, and 1158 cm^{-1}, respectively,[28] provides vastly enhanced sensitivity. Such tagging also has the advantage of producing a new carbonyl peak which is easily resolved from that of the MUIN carbonyl.

This new carbonyl stretch affords a forthright measurement of surface coverage. In order to test this strategy, the integrated areas of the carbonyl peak in TFAA-tagged monolayers of 11-mercaptoundecanol (MUTFA) at different fractional surface coverages were compared. Monolayers of 11-mercaptoundecanol in decanethiol, $\theta_{OH} = 1.0$ and $\theta_{OH} = 0.5$, were tagged with TFAA. The resulting integrated carbonyl areas, normalized to the methylene-stretching area, for $\theta_{OH} = 1.0$ were twice those for $\theta_{OH} = 0.5$. The carbonyl fwhm for $\theta_{OH} = 1$ is 38 cm^{-1}, versus 20 cm^{-1} for $\theta_{OH} = 0.5$. Certainly, at higher fractional surface coverages, there are a wider range of carbonyl orientations and interactions; however, on the basis of these results, it appears that even at high fractional surface coverage there is no sizable fraction of the carbonyls oriented parallel to the surface. Analysis of the integrated carbonyl areas for MUIN monolayers in decanethiol at various fractional surface coverages shows similar results.

Incorporation of pentaammineruthenium(II) into the outer plane of the monolayer simultaneously introduces a large, positive charge and allows for *in situ* electrochemical monitoring of hydrolysis. Such tagging also allows the total charge at the monolayer outer plane to be varied potentiostatically.

Ruthenium can be attached to MUIN either before or after monolayer formation. There are advantages associated with either approach. With preassembled monolayers, the overall structure of the monolayer can be more easily determined prior to ruthenium tagging. Of course, introduction of the ruthenium may change the local structure at the outer plane of the monolayer but is unlikely to change the overall packing of the inner monolayer, especially in coassembled systems where the underlying alkane chain packing is governed by an unsubstituted alkanethiol. The thermodynamics of competitive adsorption, never straightforward to calculate *a priori*, are more easily understood or rationalized when there is no charge on adsorbates. Alternatively, tagging prior to monolayer formation most likely provides a different, more diffuse underlying monolayer structure and holds the promise of higher ruthenium loadings.

The loading of ruthenium obtained with preassembly tagging is identical to that obtained in similar systems; an electroactive coverage of 2×10^{-10} mol cm^{-2} corresponds to a close-packed monolayer of $[Ru(NH_3)_5(py)]^{2+}$, or $\theta_{Ru} = 1$.[29] Even at this coverage, the ruthenium centers act independently, as illustrated by the cyclic voltammogram shown in Figure 4a. The maximum attainable ruthenium loading with postassembly tagging, 5×10^{-11} mol cm^{-2}, corresponds to $\theta_{Ru} = 0.25$. At this level of surface coverage every ruthenium center has, on average, four closest

(28) Redington, R. L. *Spectrochim. Acta* **1975**, *31A*, 1699.

(29) (a) Finklea, H. O.; Hanshew, D. D. *J. Am. Chem. Soc.* **1992**, *114*, 3173. (b) Finklea, H. O.; Hanshew, D. D. *J. Electroanal. Chem.* **1993**, *347*, 327. (c) Finklea, H. O.; Ravenscroft, M. S.; Snider, D. A. *Langmuir* **1993**, *9*, 223.

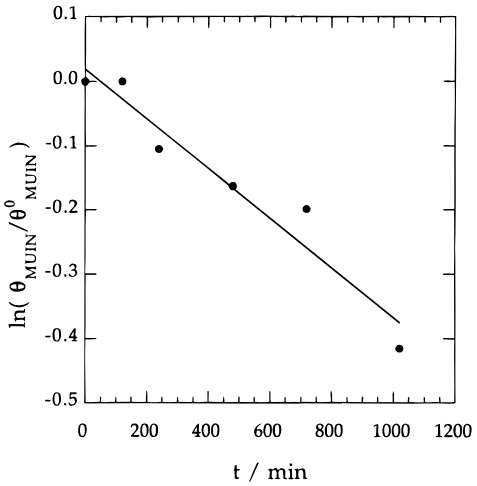

Figure 5. Hydrolysis at pH 10 of MUIN diluted in a monolayer of decanethiol, $\theta^{\circ}_{MUIN} = 0.25$, as monitored by TFAA tagging of the resultant surface-confined alcohol and subsequent infrared reflection−absorption spectroscopy.

Table 1. Pseudo-First-Order Rates of Ester Hydrolysis for MUIN Monolayers

θ_{MUIN}	μ/mM	$k'/10^{-3}$ min^{-1}
1	2	<0.001
0.25	2	0.2

ruthenium neighbors among the six available sites in a hexagonal closest-packed structure.

Incomplete ruthenium decoration of the monolayer could be due to coulombic repulsions, or to a limited number of accessible isonicotinates in a preassembled monolayer. In order to address this question, monolayers of MUIN diluted in decanethiol were prepared, with θ_{MUIN} ranging from 0.05 to 1.0, as estimated via IR spectroscopy. When these monolayers were tagged with ruthenium, Γ_{Ru} tracked θ_{MUIN} at low values of θ_{MUIN}, but as θ_{MUIN} increased beyond 0.1, Γ_{Ru} remained constant at 5×10^{-11} mol cm^{-2}. We believe these results implicate coulombic repulsion as the operative barrier to high Γ_{Ru} values on preassembled monolayers.

The kinetics of electron transfer in ruthenium-tagged MUIN monolayers match those reported for amide-linked $[Ru(NH_3)_5(py)]^{2+/3+}$ at this distance above gold electrodes[29] and are independent of the method selected for ruthenium tagging.

MUIN multilayers also can be tagged with ruthenium after multilayer deposition, leading to Γ_{Ru} values as large as 2×10^{-8} mol cm^{-2}. Cyclic voltammograms of tagged multilayer systems show a ΔE_p of 59 mV at low scan rates, which is characteristic of diffusion-limited systems.

Monolayer Hydrolysis. Monolayers with $\theta_{MUIN} = 1.0$ were hydrolyzed in buffered aqueous pH 10.0 solutions for periods ranging from 2 to 72 h prior to TFAA tagging. At short reaction times no hydrolysis was observed. Even at the longest times monitored, no more than 5% of the MUIN hydrolyzed (Table 1).

MUIN monolayers still block ion penetration after prolonged hydrolysis times. Fractional pinhole coverages, $1 - \theta$, after hydrolysis were typically 4×10^{-3}, as measured by ac impedance spectroscopy. Such results preclude significant loss of monolayer coverage during the extensive times in contact with basic aqueous solutions.

When MUIN is diluted in decanthiol such that $\theta_{MUIN} = 0.25$, hydrolysis proceeds much more quickly, as illustrated in Figure 5. The large amount of scatter in Figure 5 can be ascribed, in part, to the practice of using different samples for each point in the plot. While somewhat unsatisfactory with respect to precision, this practice removes the cumulative influence of alternating buffer and THF reaction protocols during the course of a run.

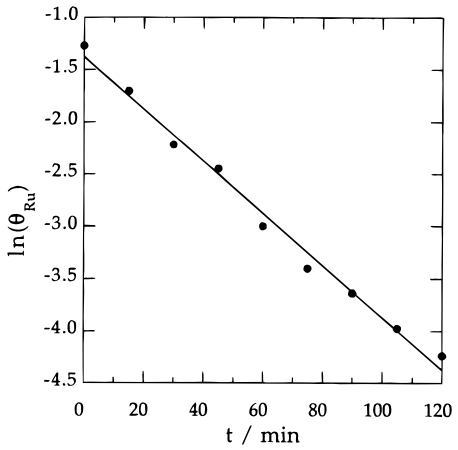

Figure 6. Hydrolysis at pH 10 of MUIN diluted in a monolayer of decanethiol and tagged after self-assembly with pentaammineruthenium(II), $\theta_{Ru} = 0.25$. Details of the CV-based hydrolysis monitoring are given in the text.

Table 2. Pseudo-First-Order Rates of Ester Hydrolysis for MUIN Monolayers Tagged with Ru^{2+}

θ_{Ru}	μ/mM	$k'/10^{-3}$ min^{-1}
1	2	~100
0.25	2	27
0.25	200	9
0.25[a]	2	0.3

[a] Control experiment with no ester linkage.

At $\theta_{MUIN} = 0.25$, there appears to be ample opportunity for hydroxide-mediated attack on the ester functionality. The initial rate of hydrolysis, using a pseudo-first-order treatment, is 0.2×10^{-3} s^{-1}.

Rates of base-mediated ester hydrolysis measured by TFAA tagging undoubtedly reflect a lower bound. The tagging reaction could be sterically hindered at isolated OH sites present in a MUIN monolayer after small degrees of reaction, producing fewer trifluoroacetates than expected. In addition, there is strong evidence that OH surfaces rearrange after long exposures to air, sequestering some of the OH into sites inaccessible to TFAA tagging.[30] The efficacy of the TFAA-tagging reaction may be less than unity, although previous work has shown that such tagging approaches 95% efficacy on fully-hydroxylated surfaces.[1] We observe no difference in spectra of TFAA-tagged monolayers of 11-mercaptoundecanol and monolayers formed from bis[11-((trifluoroacetyl)oxy)undecyl] disulfide.

Using mixed monolayers with $\theta_{MUIN} = 0.1$, ruthenium tags were attached and the monolayer was hydrolyzed at pH 10. After ester hydrolysis, the ruthenium-tagged isonicotinate diffuses into solution, where it is lost to further voltammetric interrogation. Cyclic voltammograms, recorded at intervals in pH 4 electrolyte, show this loss of electroactive signal. The resulting data, shown in Figure 6 and Table 2, provide evidence for accelerated pseudo-first-order hydrolysis of the MUIN ester linkage relative to untagged monolayers.

The results of a similar experiment, using a $\theta_{Ru} = 1$ monolayer prepared by tagging prior to assembly, are shown in Figure 7. In this experiment, the ester linkage initially hydrolyzes more quickly than at longer times. We believe this higher initial rate is related to the higher

(30) Evans, S. D.; Sharma, R., Ulman, A. *Langmuir* **1991**, *7*, 156.

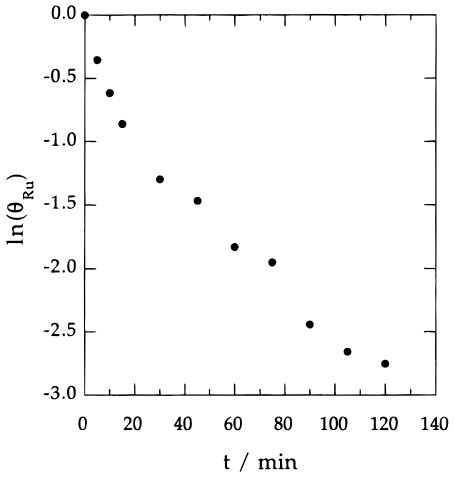

Figure 7. Hydrolysis at pH 10 of a MUIN monolayer tagged prior to self-assembly with pentaammineruthenium(II), $\theta_{Ru} = 1.0$. Details of the CV-based hydrolysis monitoring are given in the text.

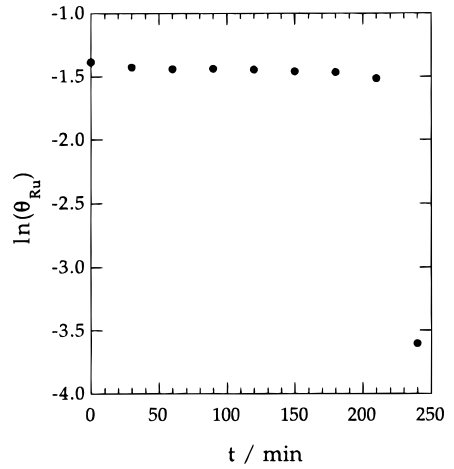

Figure 8. Stability at pH 10 of a monolayer of 4-(12-mercaptododecyl)pyridine diluted in decanethiol and tagged after self-assembly with pentaammineruthenium(II), $\theta_{Ru} = 0.25$. Details of the CV-based stability monitoring are given in the text.

charge density on the outer plane of the monolayer at short times, a phenomenon discussed in greater detail below.

In electrochemically-tagged hydrolysis experiments it is necessary to distinguish among loss of ruthenium by hydrolysis of the MUIN ester linkage, decomposition of the pendant ruthenium complex at pH 10, and loss of electroactive complex by desorption of the entire alkanethiol from the gold surface. With regard to the second of these potential loss mechanisms, spectrophotometric control experiments show the free isonicotinate ruthenium complex, $[Ru(NH_3)_5(NC_5H_4CO_2)]^+$, to be stable over a pH range of 10−13 for periods in excess of 4 h if oxygen is excluded. In addition, the surface-confined Ru(II) complex is stable at pH 4 to within a few percent for times exceeding 1 h. Hence, ruthenium loss by decomposition of the transition metal complex seems minimal. To investigate the third potential mechanism for ruthenium loss, control hydrolyses were performed using monolayers of 4-(12-mercaptododecyl)pyridine, which has no ester linkage. Results typical of these experiments are shown in Figure 8. The monolayer is stable for a few hours, followed by a rapid loss of electroactive ruthenium. Retreatment with the tagging protocol following ruthenium loss does not produce additional electroactive ruthenium. AC impedance and CV estimates of $1 - \theta$ on monolayers after ruthenium loss show that a large fraction of the gold surface is accessible to solution-phase redox species. We believe the loss of ruthenium after prolonged exposure is due to massive breakdown of the monolayer, whereby the entire ruthenium−alkanethiol complex leaves the gold surface. In support of this interpretation, theoretical calculations show that charge-bearing monolayers immersed in a solvent of high dielectric constant are much less stable than monolayers bearing no charge.[31] The sample-to-sample variability in the time to breakdown most likely reflects the distribution and density of defect sites between these monolayers. Thus, while catastrophic desorption of the entire alkanethiol may occur after long exposure times, we believe the pseudo-first-order loss of ruthenium at short times shown in Figures 6 and 7 is due to hydrolysis of the MUIN ester linkage.

A number of factors affect the rate of base-mediated ester hydrolysis at the monolayer/solution interface. In the case of MUIN monolayers bearing no affixed charge, the increase in hydrolysis rate observed when moving from $\theta_{MUIN} = 1$ monolayers to $\theta_{MUIN} = 0.25$ monolayers can be ascribed to the increased access of hydroxide ion to the ester carbonyl carbon. Upon incorporation of fixed, positive charge at the monolayer/solution interface, the increased hydrolysis rate can be understood in terms of the structure of the diffuse double layer.

The double layer can be modeled roughly as a two-plate capacitor, comprised of the MUIN monolayer and the diffuse layer of charge in solution. Any charge residing on the monolayer outer plane is balanced by the charge in some thickness of adjacent solution. Monolayer/solution interfaces are particularly well-suited to the Gouy−Chapman model,[32] especially as concerns the differential capacitance of such systems.[33] In a similar fashion, shifts in the formal potential of pendant, charged electroactive species can be related to the Donnon potential at the monolayer/solution interface.[11] The electrostatic potential, ψ, between the monolayer surface and the bulk of solution can be calculated from Gouy−Chapman theory as

$$\psi = \frac{2kT}{ze} \sinh^{-1}\left(\frac{\sigma^M}{(8kT\epsilon\epsilon_0 C)^{1/2}}\right)$$

where σ^M is the charge density at the monolayer surface and C is the concentration of electrolyte. The value of σ^M in the ruthenium-tagged MUIN system is $2F\Gamma_{Ru}$, if we assume that all the charge on the interface is associated with Ru^{2+}. This electrostatic potential induces a shift in the localized pH, equal to $F\psi/2.3RT$, as hyroxide ions are preferentially ordered close to the plane of ruthenium attachment. In the current example, a monolayer containing $\Gamma_{Ru} = 5 \times 10^{-11}$ mol cm^{-2} and $z = 2+$ immersed in a pH 10 buffer with total ionic strength of $C = 2$ mM yields $\psi = 126$ mV, which is equivalent to a 2.1 pH unit increase in local pH. Table 3 shows expected values of ΔpH for various surface loadings and electrolyte concentrations.

By using relatively high surface loadings of highly-charged species immersed in dilute electrolytes, the local pH can be substantially augmented. This is illustrated in Figure 7, where fully three-quarters of the initial charge on the interface is lost in the first 20 min, only to have the rate of hydrolysis decrease in response to the lower charge-

(31) Doblhofer, K.; Figura, J.; Fuhrhop, J.-H. *Langmuir* **1992**, *8*, 1881.
(32) Bard, A. J.; Faulkner, L. R. *Electrochemical Methods*; John Wiley & Sons: New York, 1980.
(33) Mith, C. P.; White, H. S. *Langmuir* **1993**, *9*, 1.

Table 3. Interfacial Potentials (ψ), Calculated by Gouy−Chapman Theory, as a Function of the Charge on the Complex (z^M), Surface Coverage of a Pendant Metal Complex (Γ), and Electrolyte Concentration (C)

z^M	$\Gamma/10^{-10}$ mol cm^{-2}	C/mM	ψ/mV	ΔpH[a]
+2	2.0	200	138	2.3
+2	2.0	20	197	3.3
+2	2.0	2	256	4.3
+2	0.5	200	70	1.2
+2	0.5	20	126	2.1
+2	0.5	2	185	3.1
+3	2.0	200	159	2.7
+3	2.0	20	218	3.7
+3	2.0	2	277	4.7
+3	0.5	200	89	1.5
+3	0.5	20	147	2.5
+3	0.5	2	206	3.5

[a] The resultant change in local pH at the interface, equal to $F\psi/2.3RT$.

induced pH shift. Additional experiments confirm that the increase in localized pH cannot be salted-out entirely by use of high concentrations of electrolyte (Table 2).

Chemistry of Ruthenium at the Monolayer/Solution Interface. Attempts to tag existing MUIN monolayers using aqueous solutions of $[Ru(NH_3)_5(OH_2)]^{2+}$ were largely unsuccessful, producing at most 2% surface coverage. Results were identical when using $[Ru(NH_3)_5(OH_2)]^{2+}$ prepared fresh from Jones reduction[34] or from fresh, solid hexafluorophosphate salt. Variation of the pH from 3 to 10 and the ionic strength from 0.1 to 3 M (with LiCl) produced identical results. However, use of a suitable, nondonating solvent, such as THF, produced surface loadings of $\Gamma_{Ru} = 5 \times 10^{-11}$ mol cm^{-2}. This contrasts with surface loadings of $\Gamma_{Ru} = 2 \times 10^{-10}$ mol cm^{-2} obtained when the ruthenium is affixed before monolayer assembly.

The general failure of the aqueous-based tagging is puzzling. The substitution of pyridine for water in $[Ru(NH_3)_5(OH_2)]^{2+}$ is strongly favored, with an equilibrium constant[35] of 2.4×10^7. As shown earlier in the contact angle measurements, the pK_a of the surface-confined pyridine residues is 5.5; use of buffered pH 7 solutions for attachment should produce surfaces free of pyridinium. Even at lower pH, where the pyridine residues are protonated, the rate constant for ligand substitution[35] only decreases by a factor of 30.

The reason for poor performance in affixing ruthenium could have its basis in the mechanism of ligand substitution. Kinetics studies on $[Ru(NH_3)_5(OH_2)]^{2+}$ ligand substitution support an S_N1 mechanism, whereby the coordinated water is expelled, leaving a five-coordinate intermediate prior to pyridine insertion.[35] Given the loss of at least four degrees of freedom upon tethering isonicotinate, properly positioning the five-coordinate intermediate for isonicotinate insertion could be sluggish on the time scale of reaquation. The use of THF solvent promotes formation of a solvato complex, altering the stability of the five-coordinate intermediate. Alternatively, THF could induce changes in monolayer structure, providing a change in orientation or more freedom of movement for the tethered isonicotinate relative to that in water. At present, we have no means to discriminate between mechanistic and structural control of this system.

In an attempt to access even larger ester hydrolysis rates via increased charge on the monolayer surface, hydrolysis runs at pH 10 were attempted using ruthenium-tagged MUIN monolayers under potentiostatic control at +0.4 V versus SCE. Under these conditions, the pendant ruthenium complexes are oxidized to Ru(III) and bear a charge of +3. In such experiments all electroactive ruthenium disappears within 30 s. In CV experiments at pH 10, the decay of electroactive ruthenium is proportional to the time spent as Ru(III). A representative cyclic voltammogram of ruthenium-tagged MUIN at pH 10 is shown in Figure 4b. After partial destruction of ruthenium via a few cycles at high scan rates, the electrode could be returned to pH 4 solution, with the recovery of a more normal cyclic voltammogram, albeit with lower surface coverage. These monolayers could be retagged with ruthenium, producing surface coverages equivalent to those initially present.

Given that monolayers damaged by cycling in pH 10 solutions can be retagged, the loss mechanism does not involve ester hydrolysis. We believe the loss of electroactivity is due to the disproportionation of Ru(III) in basic environments. Rudd and Taube showed that pentaamminepyridineruthenium(III) complexes disproportionate to Ru(II) and Ru(IV) in basic environments.[36] They found the rate of disproportionation to be pH dependent, with 50% loss of Ru(III) over a period of 90 min at pH 10.

The accelerated rate of disproportionation evidenced in our system can be ascribed to two phenomena. The increase in the localized pH, as discussed above, enhances the deprotonation and eventual destruction of the Ru(IV) product. Since the Ru(IV) complex is a better acid than either the corresponding Ru(II) or Ru(III) complex, the more efficient removal of a proton from an amine coordinated to Ru(IV) will shift the mass balance toward greater disproportionation. Secondly, the use of potentiostatic control induces a "redox pumping" of the Ru(IV) species. In homogeneous solution, exactly half of the Ru(III) which disproportionates becomes Ru(II), which undergoes no further reaction. In our system, Ru(II) formed by disproportionation is immediately oxidized by the electrode to Ru(III), which disproportionates again. In this fashion, all the Ru(III) on the surface is quickly converted to Ru(IV), which suffers accelerated loss via a localized pH-enhanced deprotonation.

Conclusions

The rates of reactions at well-ordered surface sites can differ significantly from those of similar reactions in homogeneous solution. Monolayer assemblies, by virtue of their orderliness, provide ideal systems for exploring these differences. Steric effects can control ion and solvent access to sites within the monolayer at high surface coverages; the degree of solvent access to the reaction site can be controlled by the lateral composition of the monolayer. Fixation of charge at the monolayer/solution interface can also be used to control pH-sensitive reactions at sites adjacent to this interface. Gouy−Chapman double-layer theory provides a basic understanding of the extent of control available via this mechanism.

Acknowledgment. Acknowledgment is made to the donors of The Petroleum Research Fund, administered by the ACS, for partial support of this research. Fellowships were provided by an NSF-Research Experiences for Undergraduates site award to Harvey Mudd College, NSF REU CHE-9322804, and a Jean Dreyfus Boissevain Undergraduate Scholarship. H.V.R. acknowledges helpful discussions with Mark S. Wrighton during a sabbatical leave spent in his laboratory.

LA960027P

(34) Ford, P.; Rudd, De F. P.; Gaunder, R.; Taube, H. *J. Am. Chem. Soc.* **1968**, *90*, 1187.

(35) Shepherd, R. E.; Taube, H. *Inorg. Chem.* **1973**, *12*, 1392.

(36) Rudd, De F. P.; Taube, H. *Inorg. Chem.* **1971**, *10*, 1543.